eISSN (Online): 2598-0580

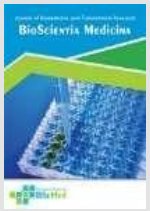

Bioscientia Medicina: Journal of Biomedicine & Translational Research

Journal Homepage: www.bioscmed.com

Utility of Tc-99m DTPA Hybrid SPECT/CT Cisternography in the Detection of Occult Postoperative CSF Fistula in an Infant with Lipomeningomyelocele: A Diagnostic Challenge and Technical Considerations

I Kadek Herry Hermawan[1*], Achmad Hussein Sundawa Kartamihardja[1], Trias Nugrahadi[1], Reza Rinaldy Harahap[1]

[1]Department of Nuclear Medicine and Molecular Theranostics, Faculty of Medicine, Universitas Padjadjaran/Dr. Hasan Sadikin General Hospital, Bandung, Indonesia

ARTICLE INFO

Keywords:
Cerebrospinal fluid leak
Hybrid SPECT/CT
Lipomeningomyelocele
Pediatric nuclear medicine
Tc-99m DTPA

***Corresponding author:**
I Kadek Herry Hermawan

E-mail address:
herryhermawan.nm@gmail.com

All authors have reviewed and approved the final version of the manuscript.

0https://doi.org/10.37275/bsm.v10i4.1550

A B S T R A C T

Background: Lipomeningomyelocele represents a complex spectrum of closed spinal dysraphism where surgical repair is frequently complicated by cerebrospinal fluid leakage. While overt fistulas are clinically apparent, occult or intermittent leaks in the pediatric population pose a severe diagnostic challenge. Magnetic resonance imaging, despite being the anatomical gold standard, frequently fails to distinguish active extravasation from postoperative seroma or edema due to overlapping signal intensities. This study evaluates the diagnostic superiority of Tc-99m DTPA Hybrid SPECT/CT cisternography in resolving this dilemma. **Case presentation:** A 5-month-old female underwent resection of a large lumbosacral lipomeningomyelocele. Postoperatively, she developed persistent, clear fluid discharge from the incision, suggestive of a fistula, yet initial surgical re-exploration was inconclusive. The patient underwent radionuclide cisternography using 37 MBq of intrathecal Tc-99m DTPA. Standard planar scintigraphy at 1 hour and 3 hours was equivocal due to background renal activity. However, Hybrid SPECT/CT performed at 3 hours precisely localized an abnormal radiotracer tract extending from the thecal sac at L5 into the right multifidus muscle, a finding invisible on conventional imaging. **Conclusion:** The integration of physiological flow data from scintigraphy with the anatomical specificity of low-dose CT allows for the detection of slow-flow, occult leaks that evade MRI. In infants with distorted post-surgical anatomy, Hybrid SPECT/CT should be elevated from a problem-solving tool to a primary diagnostic modality when clinical suspicion persists. The technique facilitates targeted repair, minimizing morbidity in this vulnerable population.

1. Introduction

The clinical management of spinal dysraphism remains one of the most intricate and demanding frontiers in modern pediatric neurosurgery, representing a convergence of embryological complexity, surgical precision, and long-term functional preservation.[1] Among the spectrum of closed neural tube defects, Lipomeningomyelocele (LMM) stands out as a distinct and particularly challenging entity. Characterized by a subcutaneous lipomatous mass that extends through a vertebral bony defect to attach directly to the spinal cord, LMM is not merely a cosmetic anomaly but a profound structural tethering of the central nervous system. The pathophysiology of this condition traces back to the earliest stages of gestation, specifically the failure of primary neurulation. During the fourth week of embryonic development, a critical event known as premature disjunction occurs, where the cutaneous ectoderm separates from the neuroectoderm before

the neural tube has successfully closed. This premature breach allows pluripotent mesenchymal cells to invade the developing neural canal. These cells subsequently differentiate into lipomatous tissue that becomes inextricably woven into the dorsal aspect of the spinal cord, often infiltrating the central canal and enveloping the dorsal nerve roots. This anatomical reality creates a fixed point of attachment, or tether, which prevents the normal cephalad migration of the spinal cord as the vertebral column elongates during fetal growth. The resulting traction on the conus medullaris leads to the clinical syndrome of tethered cord, characterized by progressive ischemic injury to the neural elements, resulting in lower limb paresis, sensory deficits, and neurogenic bladder or bowel dysfunction.[2]

The standard of care for LMM dictates early neurosurgical intervention, typically within the first few months of life, to untether the spinal cord and arrest the progression of neurological deterioration.[3] However, the surgical objective is fraught with a unique technical dilemma that predisposes these infants to postoperative complications. Unlike the repair of a simple meningocele, where the sac can be ligated and the dura closed easily, the repair of LMM requires the surgeon to navigate the chaotic interface between the lipoma and the functional neural placode. Because the lipoma infiltrates the neural tissue, a total resection is functionally impossible without inflicting catastrophic injury to the functional nerve roots embedded within the fat. Consequently, the neurosurgical consensus advocates for a subtotal resection, wherein the bulk of the lipoma is debulked to relieve tension, but a thin strip of lipoma is intentionally left attached to the neural placode to preserve function. This necessary surgical compromise creates a significant challenge for dural closure. The native dura in patients with LMM is often dysplastic, thin, friable, and anatomically deficient. Furthermore, the residual lipomatous tissue on the placode can physically impede the approximation of the dural edges. When combined with the lack of robust paraspinal musculature and distinct fascial layers in infants to buttress the repair, the creation of a watertight dural seal becomes exceptionally difficult.

It is within this context of compromised tissue integrity and complex reconstruction that cerebrospinal fluid (CSF) leakage emerges as a pervasive and dreaded complication. The incidence of postoperative CSF leaks in complex spinal dysraphism repair has been reported to range significantly, with some series citing rates as high as 15% in complex re-operations.[4] A postoperative CSF fistula is not merely a wound healing issue; it creates a direct, patent communication between the sterile subarachnoid space and the external environment, serving as a conduit for bacterial colonization. If left undiagnosed or untreated, these leaks can precipitate devastating sequelae, including bacterial meningitis, ventriculitis, arachnoiditis, and the formation of pseudomeningoceles that compress neural structures. The physiological consequences of a persistent leak also include intracranial hypotension, which can lead to subdural hematomas and further neurological decline. Therefore, the prompt and accurate identification of a CSF leak is an absolute imperative in the postoperative management of these vulnerable infants.

The diagnostic landscape for postoperative CSF leaks, however, is fraught with ambiguity. While a high-flow fistula presenting with a brisk, continuous discharge of clear fluid is clinically obvious, many leaks in the pediatric population are occult or intermittent. These leaks may present only as a boggy subcutaneous collection, a non-healing wound, or intermittent dampness on dressings that occurs only when the infant cries or strains. In such equivocal scenarios, clinicians turn to advanced imaging to confirm the diagnosis and, more importantly, to localize the tract for surgical revision. Magnetic resonance imaging (MRI) is universally regarded as the gold standard for defining spinal anatomy due to its superior soft-tissue contrast and lack of ionizing radiation.[5] However, in the immediate postoperative period, MRI suffers from a critical limitation in specificity regarding fluid dynamics. On standard T2-

weighted sequences, which are relied upon to visualize fluid, cerebrospinal fluid appears hyperintense (bright white). Unfortunately, the postoperative surgical bed is a chaotic environment filled with other fluids that share identical signal characteristics. Postoperative edema, seromas, dissolving hematomas, and fluid-saturated hemostatic agents such as gelatin sponges or oxidized cellulose all appear hyperintense on T2-weighted images.[6]

This overlap in signal intensity creates a diagnostic blind spot. The MRI scanner visualizes the presence of protons, specifically hydrogen nuclei, but it cannot discern the origin of those protons or their flow dynamics. A pocket of bright signal in the paraspinal muscles could represent a contained, static postoperative seroma that requires no intervention, or it could represent an active, expanding pseudomeningocele fed by a dural defect.[7] Differentiating between these two entities based on static anatomical imaging is often impossible. This limitation frequently leaves the neurosurgeon in a precarious position: either perform a blind surgical exploration of a healing wound, risking further tissue trauma and infection, or adopt a wait and see approach that risks meningitis. CT Myelography, another anatomical modality, offers higher spatial resolution for bony defects but requires the intrathecal administration of iodinated contrast media. In infants, this procedure carries non-negligible risks, including neurotoxicity, seizures, and the requirement for sedation or general anesthesia, in addition to a significant burden of ionizing radiation to the developing spine and bone marrow. Furthermore, CT Myelography provides only a temporal snapshot of the spine; if the leak is intermittent and the infant is not straining at the exact moment of image acquisition, the contrast may not extravasate, leading to a false-negative result.

In response to these diagnostic limitations, nuclear medicine offers a functional and physiological alternative through the technique of radionuclide cisternography. Unlike anatomical imaging, which relies on tissue density or proton relaxation times, radionuclide cisternography utilizes the principle of tracer kinetics and compartmentalization. The procedure involves the intrathecal injection of a radiopharmaceutical, most commonly Technetium-99m labeled Diethylenetriaminepentaacetic acid (Tc-99m DTPA). This molecule is hydrophilic, stable in CSF, and biologically inert. Once injected, it mixes freely with the CSF and diffuses throughout the subarachnoid space, mimicking the natural flow dynamics of the fluid. The diagnostic power of this modality lies in the biological exclusivity of the tracer. Under normal physiological conditions, the radiotracer should remain confined within the subarachnoid space until it is absorbed by the arachnoid granulations or cleared by the kidneys after systemic absorption. The detection of radiotracer activity outside the dural sac—within the paraspinal musculature, subcutaneous fat, or dressing material—provides definitive, unequivocal evidence of a CSF leak. The surrounding soft tissues effectively have a background signal of zero, creating an infinite contrast-to-noise ratio for the leak.[8]

Historically, radionuclide cisternography was performed using planar (two-dimensional) scintigraphy. While effective for gross leaks, planar imaging suffers from the limitations of projection radiography: the three-dimensional anatomy is collapsed into a two-dimensional image, resulting in the superimposition of structures. In small infants, where the distance between the spinal canal and the kidneys or bladder is only a few centimeters, the intense radioactivity from renal excretion can shine through and obscure faint tracer activity in the spine, leading to inconclusive results.[9] The evolution of this technique into Hybrid Single-Photon Emission Computed Tomography/Computed Tomography (SPECT/CT) has revolutionized the field. SPECT/CT combines the high physiological sensitivity of the radiotracer with the precise anatomical localization of Computed Tomography in a single, fused examination. By rotating the gamma camera detectors 360 degrees around the patient, SPECT acquires volumetric data that allows for the mathematical separation of the

spine from the bladder and kidneys in three-dimensional space. The integrated CT component then provides a structural roadmap, allowing the interpreting physician to pinpoint the exact anatomical location of the tracer accumulation—whether it is in a nerve root sleeve, a fluid collection in the muscle, or a tract extending to the skin.

Despite the proven utility of SPECT/CT in adult populations, literature regarding its application in infants, particularly those under one year of age with complex spinal dysraphism, remains exceptionally scarce. The pediatric population presents unique challenges, including the need for specialized sedation-free immobilization protocols, precise radiation dosimetry calculations to adhere to the ALARA (As Low As Reasonably Achievable) principle, and the interpretation of images in extremely small anatomical volumes where partial volume effects are magnified. Most established protocols are derived from adult data, leaving a significant knowledge gap regarding the optimization of this modality for infants.[10] This study aims to address this gap by demonstrating the superior diagnostic accuracy of Tc-99m DTPA Hybrid SPECT/CT in identifying occult, anatomically ambiguous leaks in infants. Furthermore, we seek to establish a comprehensive, reference-quality technical protocol for pediatric cisternography that balances the need for diagnostic precision with the imperative of radiation safety, advocating for the early integration of this hybrid modality to minimize morbidity and guide precise, targeted surgical revision in this vulnerable patient population.

2. Case Presentation

The case involves a 5-month-old female infant who was referred to the Department of Neurosurgery at a tertiary care academic medical center. The infant was brought by her parents with the chief complaint of a congenital mass located in the lower back. According to the comprehensive history obtained from the parents, the mass had been present since birth. Initially, the parents described the lesion as being approximately the size of a chicken egg. However, over the subsequent five months of life, the mass exhibited a trajectory of progressive enlargement that appeared to outpace the somatic growth of the child. This rapid increase in size, combined with the cosmetic deformity, prompted the referral for neurosurgical evaluation.

The obstetric and birth history was meticulously reviewed to identify any predisposing factors. The infant was born at term, at 38 weeks of gestation, via cesarean section which was indicated due to maternal dystocia. The birth weight was recorded at 3.0 kg, which is appropriate for gestational age. The antenatal history was notable for regular prenatal care visits. The mother reported adherence to standard nutritional protocols, including the intake of folic acid supplementation during the periconceptional period and throughout the first trimester. There was no history of maternal diabetes, exposure to known teratogens, or febrile illnesses during the pregnancy. Furthermore, a detailed pedigree analysis revealed no family history of neural tube defects, spinal dysraphism, or other genetic anomalies, suggesting a sporadic occurrence of the condition. At the time of presentation to our service, the infant weighed 6.2 kg and was meeting appropriate developmental milestones for her age, including social smiling, head control, and early reaching behavior. Figure 1 summarizes the detailed chronology data of the patient.

A systematic and thorough physical examination was conducted to assess the extent of the lesion and its impact on the infant's neurological status. On general inspection, the infant appeared active, alert, and well-nourished, with stable vital signs. The local examination of the back revealed a large, soft, non-tender mass situated in the lumbosacral region, extending across the midline. The mass measured approximately 16 cm × 14 cm × 5 cm. Palpation confirmed a lipomatous consistency, characteristic of subcutaneous fat, distinct from the fluctuance of a pure meningocele.

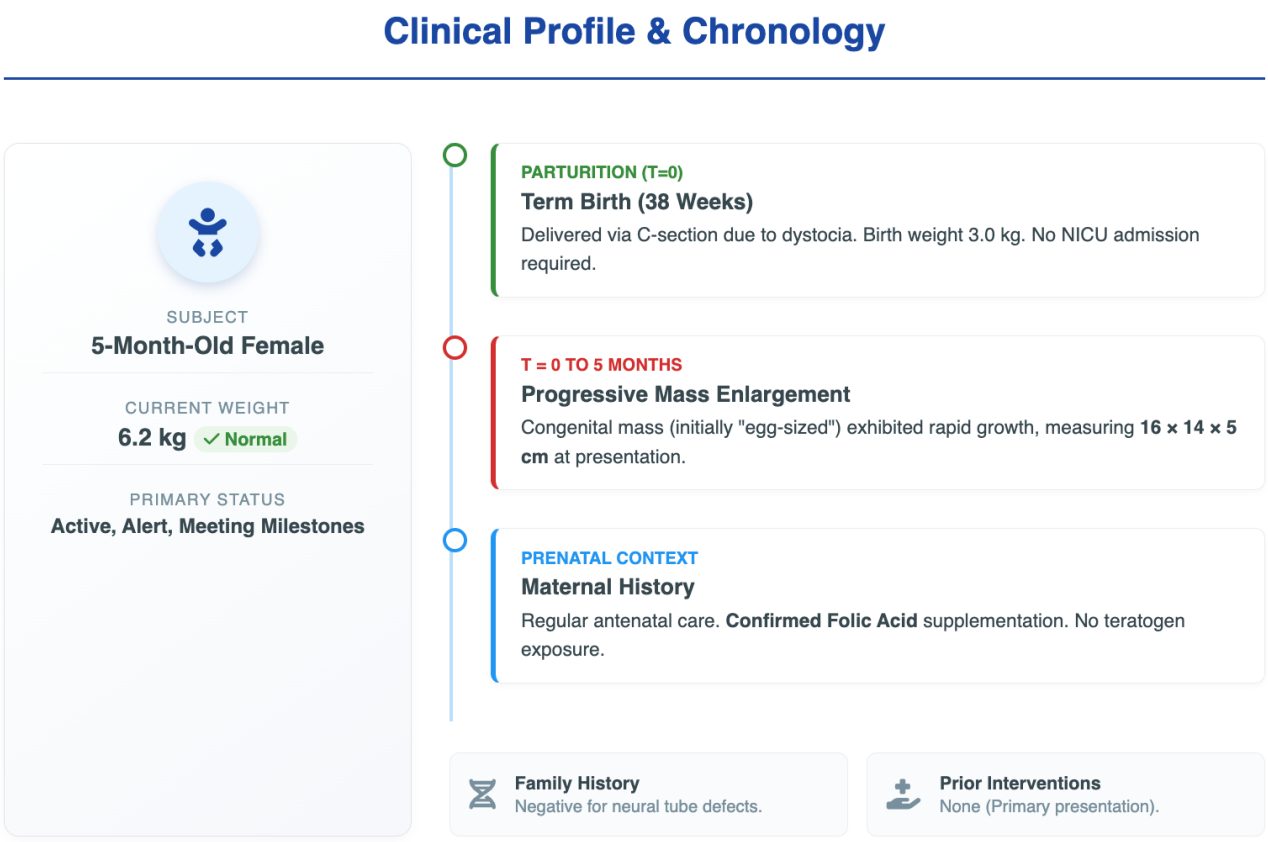

Figure 1. Clinical profile and chronology.

The overlying skin was intact and fully epithelialized, with no evidence of ulceration, inflammation, hemangioma, or hypertrichosis (fawn's tail). A central cutaneous indentation or dimple was noted at the apex of the mass, a stigma often associated with the attachment of the neural placode to the subcutaneous tissues. Importantly, there was no active discharge of fluid or purulence from the mass at the time of the initial examination.

The neurological assessment was critically important to establish a baseline prior to surgical intervention. Despite the size of the lesion, the infant demonstrated remarkably preserved neurological function. Motor examination revealed normal muscle tone in all four extremities. Spontaneous movements were symmetrical and vigorous, with antigravity strength (5/5 power) noted in the bilateral lower extremities. There was no evidence of atrophy or fasciculations. Sensation appeared intact, as the infant withdrew equally to tactile stimuli in all dermatomes of the lower limbs. Deep tendon reflexes, including the patellar and Achilles reflexes, were present and symmetric. Primitive reflexes, including the Moro and grasp reflexes, were intact and age-appropriate. Examination of the perineal region revealed a normal-appearing anal wink reflex, and the anal sphincter tone was judged to be normal upon gross examination, suggesting preserved sacral nerve function. The bladder was palpable but not distended, and the parents reported intermittent voiding with a good stream, arguing against gross neurogenic bladder dysfunction at this stage. The detailed findings of the clinical examination are presented in Figure 2.

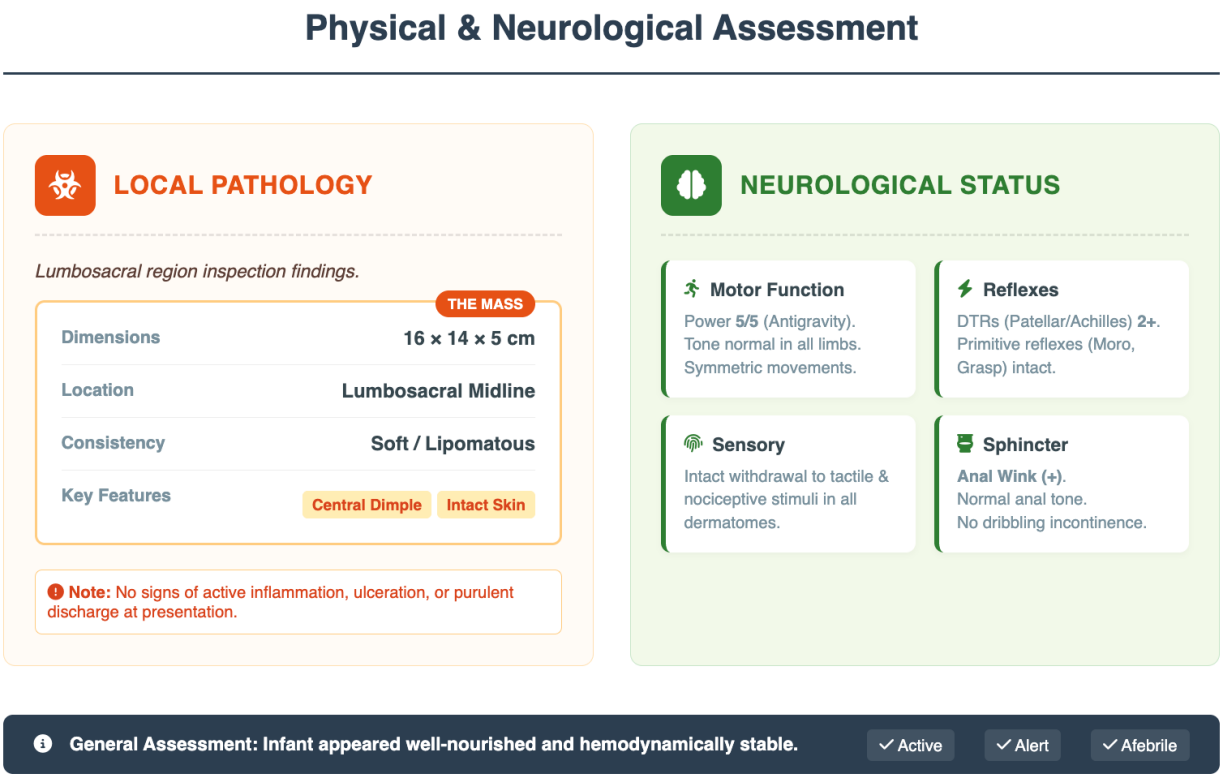

Figure 2. Physical and neurological assessment.

Following the clinical assessment, the patient underwent magnetic resonance imaging (MRI) of the spine to delineate the anatomy. The MRI confirmed the diagnosis of a complex lipomeningomyelocele. The imaging revealed a large subcutaneous lipoma extending through a dorsal bony defect (spina bifida) in the lumbosacral vertebrae. The lipoma was seen to penetrate the dura and merge with the dorsal aspect of the spinal cord, resulting in a low-lying conus medullaris (tethered cord) at the L4-L5 level. Based on these findings and the progressive enlargement of the mass, elective surgical intervention was indicated to untether the spinal cord and prevent future neurological deterioration.

The patient was taken to the operating room and placed in the prone position under general anesthesia. A midline vertical incision was made over the lumbosacral mass. The surgical strategy involved a meticulous dissection to separate the lipoma from the surrounding subcutaneous tissues. The stalk of the lipoma was traced through the lumbofascial defect. Under microscopic magnification, the dura was opened, revealing the interface between the lipoma and the neural placode. Intraoperative nerve stimulation was utilized to identify and protect functional nerve roots embedded within the lipoma. A subtotal resection of the lipoma was performed, leaving a thin strip of fat on the placode to avoid injury to the neural tissue, as is standard practice. The spinal cord was successfully untethered, confirming the free pulsatile movement of the cord. The most challenging phase of the operation was the dural reconstruction. Due to the width of the dural defect and the dysplastic nature of the native dura, a primary watertight closure was difficult. The dura was approximated using fine sutures, and a multilayered closure of the lumbodorsal fascia, subcutaneous tissue, and skin was performed to buttress the repair. The surgical details are outlined in Figure 3.

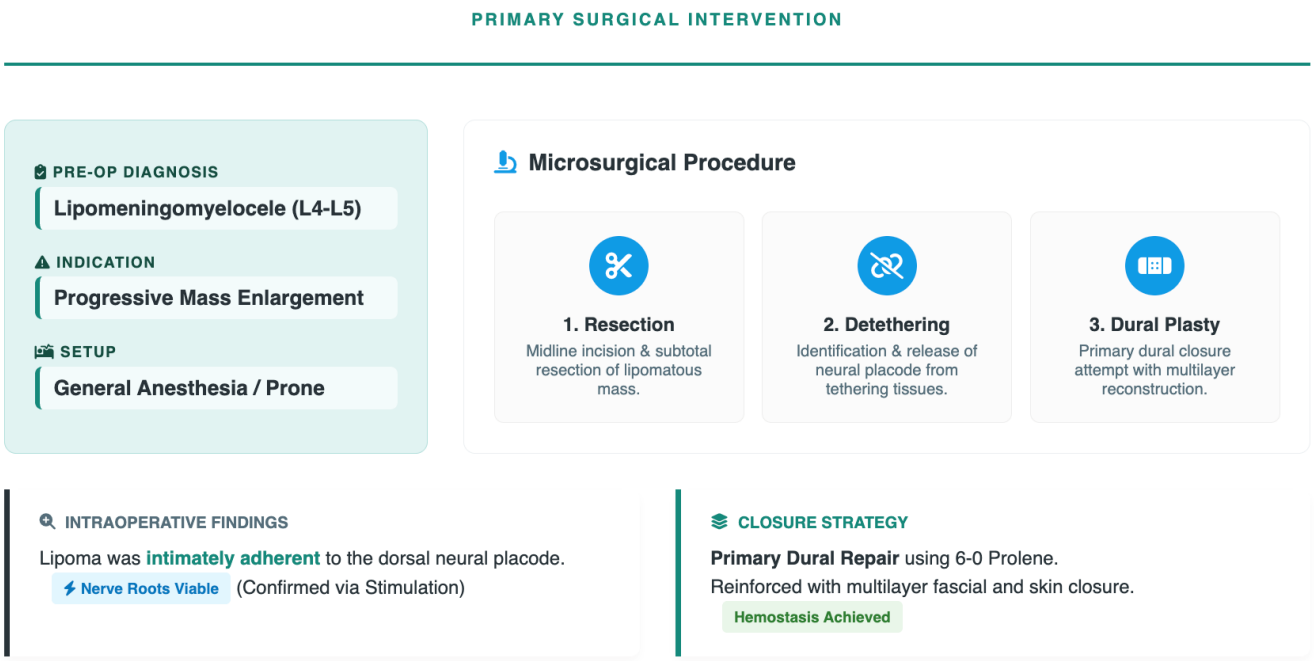

Figure 3. Primary surgical intervention.

The immediate postoperative recovery was initially unremarkable. The infant was nursed in the prone position to minimize pressure on the wound. However, on the fourth postoperative day, the nursing staff noted a persistent dampness on the surgical dressings. Upon examination, a clear, watery fluid was observed oozing from the inferior aspect of the incision site. The fluid was odorless and non-purulent. Although a Beta-2 transferrin assay—the biochemical gold standard for identifying CSF—was unavailable due to laboratory constraints, the clinical presentation was highly suggestive of a cerebrospinal fluid fistula. The appearance of the fluid, combined with the context of a recent dural repair, led to a presumptive diagnosis of a CSF leak.

Conservative management protocols were immediately initiated. The wound was reinforced with pressure dressings, and the infant was maintained in a strict prone position with the head of the bed slightly elevated to reduce hydrostatic pressure at the lumbar repair site. Acetazolamide was considered but withheld due to the patient's age and potential metabolic side effects. Despite 72 hours of rigorous conservative management, the discharge persisted, soaking through multiple dressing changes daily. On postoperative day 7, a decision was made to perform a bedside exploration of the wound under local anesthesia to inspect the closure. The exploration revealed healthy granulation tissue but failed to identify a distinct dural defect or a specific point of leakage. The tissue planes were distorted by postoperative changes, making visual identification of the fistula tract impossible. The wound was re-sutured, but the leakage recurred within 24 hours. Faced with a persistent, occult leak that could not be localized anatomically, the neurosurgical team referred the patient to the Department of Nuclear Medicine for a functional localization study. The timeline of these events is detailed in Figure 4.

Figure 4. Postoperative timeline and management.

To address the diagnostic uncertainty, a Tc-99m DTPA Radionuclide Cisternography study was meticulously planned. The protocol was designed to prioritize patient safety and image quality without the use of general anesthesia. The radiopharmaceutical used was Technetium-99m labeled Diethylenetriaminepentaacetic acid (Tc-99m DTPA). Rigorous quality control was performed using thin layer chromatography (TLC) prior to administration, confirming a radiochemical purity of greater than 98%. This high purity was essential to ensure that the tracer would remain within the CSF compartment and not contain free pertechnetate, which could degrade image quality by accumulating in soft tissues. The administered activity was 37 MBq (1 mCi), a dose calculated strictly according to the EANM (European Association of Nuclear Medicine) Pediatric Dosage Card guidelines, ensuring adherence to safety standards for a 6 kg infant. Under aseptic conditions, a lumbar puncture was performed by a senior neurosurgeon at the L3-L4 level, cephalad to the surgical site, to avoid disrupting the repair. Successful intrathecal access was confirmed by the free flow of clear CSF. The tracer was injected slowly to prevent

turbulence. Following the injection, the infant was managed using a feed and bundle technique. The child was fed 30 minutes prior to imaging to induce natural post-prandial sleep and then swaddled in a vacuum-fixation mattress. This method provided excellent immobilization for the duration of the scans, negating the need for sedation or anesthesia and their associated respiratory risks. Imaging was performed on a dual-head Hybrid SPECT/CT system (GE Discovery NM/CT 670) equipped with Low Energy High Resolution (LEHR) collimators. Static planar images were acquired at 15 minutes, 60 minutes, and 180 minutes post-injection in anterior, posterior, and lateral projections. At 180 minutes, a tomographic study was performed. The SPECT parameters involved a 128 x 128 matrix, 60 projections (30 per head), and 25 seconds per projection. Reconstruction was performed using the OSEM algorithm. A low-dose CT protocol was utilized for anatomical localization. The tube voltage was lowered to 80 kVp, and the current was modulated to approximately 30 mAs. This non-diagnostic CT aimed solely to provide an anatomical map for the tracer, significantly reducing the radiation dose to the infant. The planar images acquired at 15 and 60 minutes demonstrated good visualization of the spinal subarachnoid space and basal cisterns, confirming successful injection. However, in the lumbosacral region, the images were equivocal. Intense radioactivity from the urinary bladder and kidneys (due to renal excretion of DTPA) obscured the surgical site, creating a shine-through artifact that masked any potential leak. The Hybrid SPECT/CT performed at 180 minutes was transformative. The tomographic data separated the bladder activity from the spine. The fused images revealed a distinct, focal tract of abnormal radiotracer extending from the thecal sac at the level of the L5 vertebra. Crucially, the tracer was observed tracking laterally into the right multifidus muscle belly, forming a reservoir within the muscle tissue. This precise localization—invisible on planar imaging and ambiguous on MRI—identified the exact point of dural failure and the unexpected intramuscular trajectory of the fistula. The detailed protocol and findings are summarized in Figure 5.

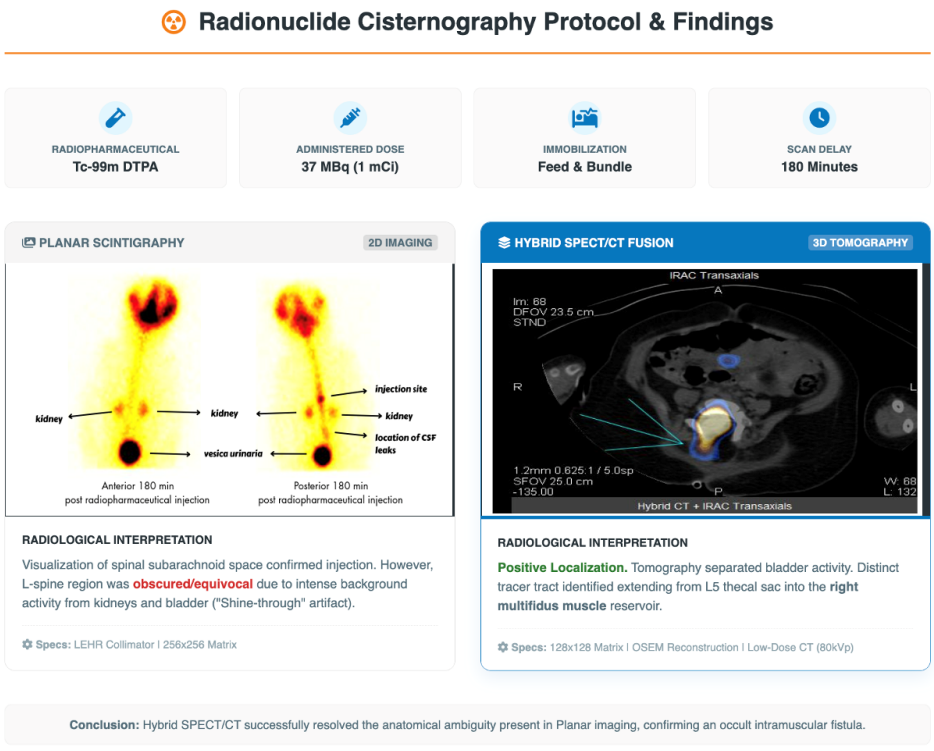

Figure 5. Radionuclide cisternography protocol and findings.

Armed with the definitive anatomical roadmap provided by the SPECT/CT study, the neurosurgical team proceeded with a targeted revision surgery. The clear localization of the leak to the right L5 level within the multifidus muscle allowed for a focused surgical approach, minimizing the need for extensive dissection. Under general anesthesia, the previous incision was reopened. Using the SPECT/CT findings as a guide, the surgeon dissected directly through the granulation tissue to the right multifidus muscle at the level of L5. Upon spreading the muscle fibers, a distinct pocket of cerebrospinal fluid (the pseudomeningocele reservoir) was encountered, exactly as predicted by the scan. Further dissection revealed a pinpoint fistulous tract in the underlying dura, which had been covered by a flap of soft tissue acting as a valve. The dural defect was refreshed and repaired using a primary suture technique. To ensure a watertight seal, the repair was reinforced with an autologous muscle patch harvested from the adjacent paraspinal musculature and secured with fibrin sealant. The wound was closed in multiple layers with meticulous attention to eliminating dead space. The postoperative course following the revision was uneventful. The clear fluid discharge ceased immediately. The infant remained afebrile, and the wound healed by primary intention. A follow-up examination at 3 months revealed a healthy, well-healed scar with no recurrence of the mass or fluid collection. Neurologically, the infant continued to develop normally with preserved motor function in the lower extremities, confirming the success of the targeted intervention. The final outcome is presented in Figure 6.

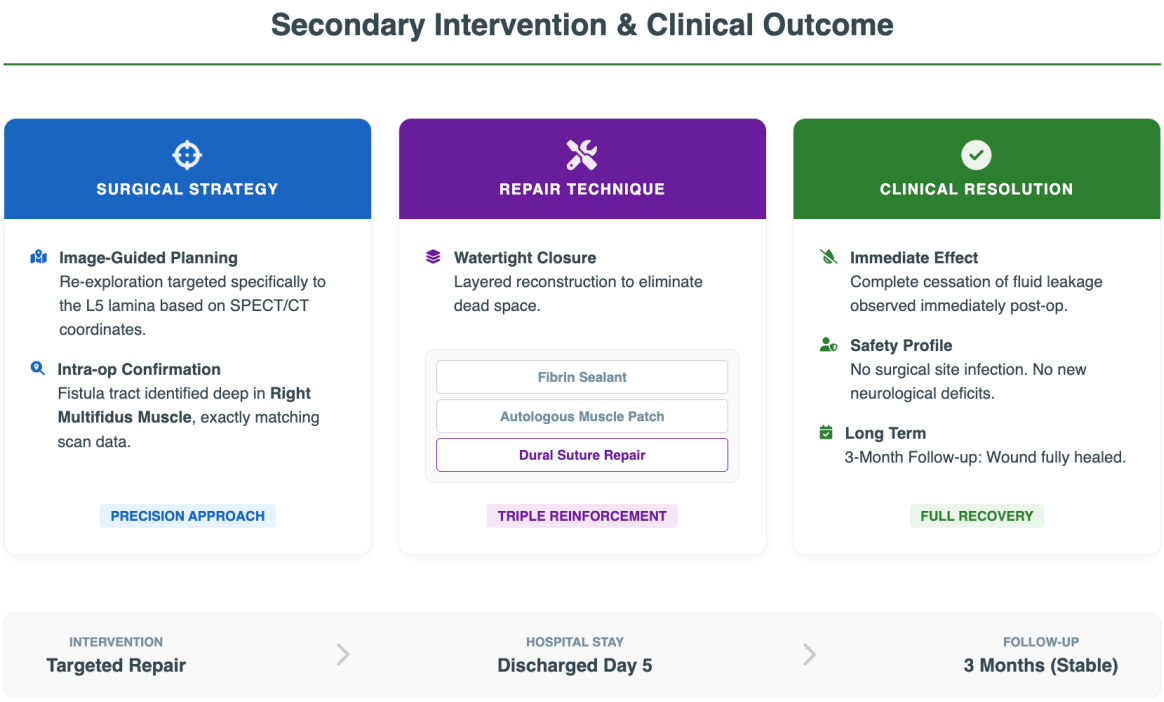

Figure 6. Secondary intervention and clinical outcome.

3. Discussion

The successful management of this case underscores the critical synergy between advanced molecular imaging and pediatric neurosurgery. The utilization of Hybrid SPECT/CT in this infant represents more than a diagnostic success; it serves as a paradigm for understanding the complex interplay between the pathophysiology of spinal dysraphism, the hydrodynamics of cerebrospinal fluid leakage, and the physics of modern imaging

modalities. Figure 7 provides an integrated overview of the causal cascade leading to persistent cerebrospinal fluid (CSF) leakage following lipomeningomyelocele repair and illustrates the mechanistic basis for the diagnostic superiority of hybrid nuclear imaging over conventional anatomical modalities in resolving these complex clinical scenarios. The flow diagram is structured into three sequential domains: the Biological Substrate (origin), the Hydrodynamic Barrier (the diagnostic challenge), and the Nuclear Resolution (the technological solution).[11] The initial panel, biological substrate, delineates the fundamental embryological and surgical factors that predispose infants to this complication. It highlights that lipomeningomyelocele results from premature disjunction during neurulation, leading to the invasion of mesenchymal adipose tissue into the developing neural tube. This results in a pathology where the lipoma is not merely an extrinsic mass but is inextricably interwoven with the functional dorsal neural placode.[12] The figure emphasizes the critical surgical consequence of this anatomy: a complete resection is functionally impossible without inflicting catastrophic neurological deficits. The neurosurgeon is compelled to perform a subtotal resection, leaving a residual lipoma-placode interface.[12] This necessary compromise, combined with the inherently dysplastic, thin, and friable nature of the native infant dura mater, results in a structurally compromised dural closure. This inherent vulnerability creates the anatomical prerequisite—a persistent weak point—for potential postoperative fistulization. The central panel transitions to the Hydrodynamic Barrier, elucidating the physiological mechanisms that render these leaks radiologically occult and challenging to detect with standard imaging. The diagram illustrates that postoperative fistulas rarely function as simple, continuous high-flow conduits in this population. Instead, they frequently operate via a dynamic ball-valve mechanism, where overlying granulation tissue, muscle fibers, or fascial flaps occlude the tract during resting states of normal intrathecal pressure. Active extravasation is often transient and intermittent, triggered only by significant spikes in intra-abdominal and intrathecal pressure, such as during crying or straining. The schematic critically contrasts this dynamic fluid physiology with the inherent limitations of magnetic resonance imaging (MRI). As depicted, MRI is fundamentally a static diagnostic modality that generates images based on proton relaxation times. Because postoperative edema, serous collections, hemostatic agents, and active CSF all possess overlapping T2 signal hyperintensities, MRI cannot definitively differentiate between static fluid accumulation in a healing wound and active, ongoing flow from a dural breach.[13] This inability to characterize flow dynamics constitutes a major diagnostic blind spot for anatomical imaging in the immediate postoperative setting. The final panel, nuclear resolution, demonstrates how the application of advanced molecular imaging principles overcomes these hydrodynamic obstacles. The figure emphasizes the paradigm shift from relying on tissue morphology to utilizing tracer kinetics. By employing Tc-99m DTPA, a hydrophilic radiopharmaceutical that accurately mimics CSF biokinetics, the diagnostic approach leverages the principle of temporal integration. Unlike the instantaneous snapshot acquisition of CT or MRI, radionuclide cisternography involves delayed imaging over several hours. This extended acquisition window allows the gamma camera to integrate counts from slow, intermittent, or low-volume extravasation that would otherwise remain sub-threshold for detection on morphological scans. Furthermore, the schematic illustrates the critical role of hybrid fusion (SPECT/CT). By mathematically coupling the high physiological sensitivity of the radiotracer distribution with the precise anatomical mapping of the low-dose CT component, the modality resolves spatial ambiguities. It definitively distinguishes normal physiological tracer activity (within nerve root sleeves) from pathological tracking into extraspinal reservoirs, such as the multifidus muscle, thereby providing the surgeon with a precise 3D roadmap for targeted intervention.[14]

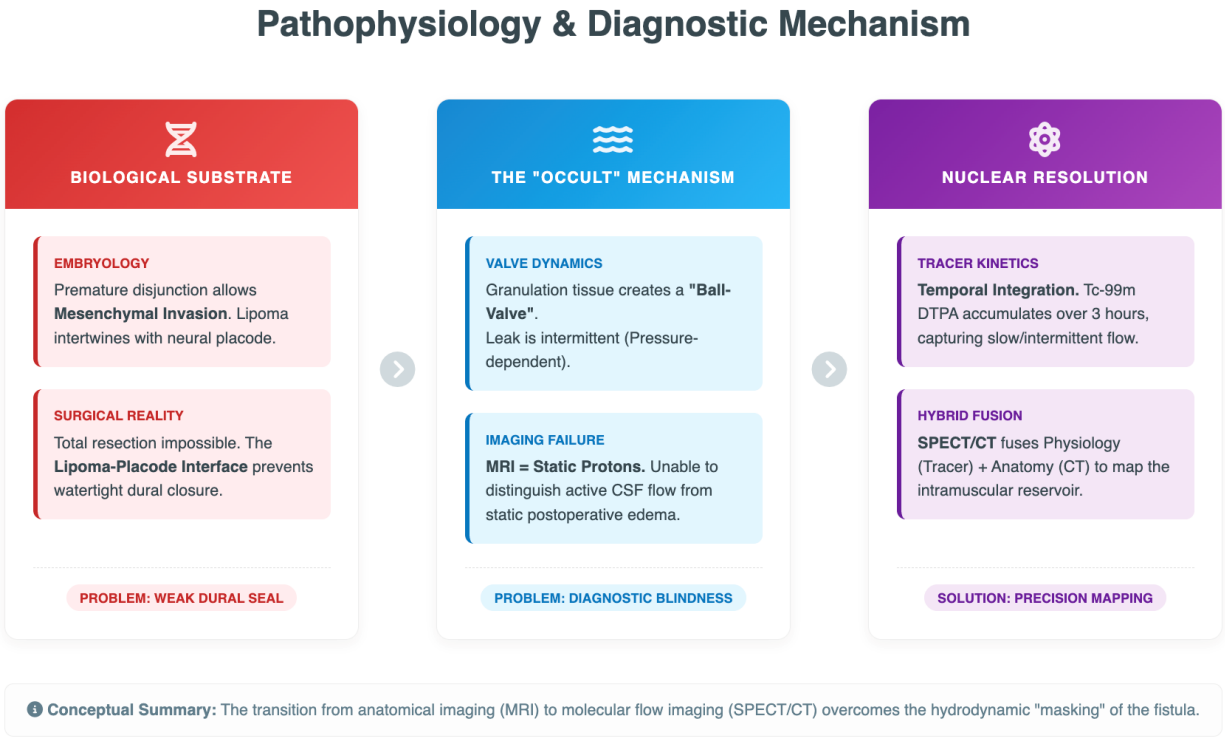

Figure 7. Pathophysiology and diagnostic mechanism.

To appreciate the complexity of the leak in this case, one must understand the anatomical substrate. Lipomeningomyelocele is a failure of primary neurulation. During the fourth week of gestation, the cutaneous ectoderm fails to separate from the neuroectoderm. This breach allows mesenchymal cells to invade the developing neural tube, preventing its closure and differentiating into lipomatous tissue.[15] Unlike a benign lipoma, this tissue is inextricably woven into the dorsal aspect of the spinal cord, often extending into the central canal. Surgically, this presents a formidable challenge. The goal of surgery is to untether the spinal cord to prevent traction ischemia, which leads to the clinical entity of tethered cord syndrome. However, total resection of the lipoma is often impossible without inflicting catastrophic injury to the functional neural placode. The neurosurgeon must perform a subtotal resection, leaving a strip of lipoma on the placode. This residual lipoma-placode interface creates a geometric mismatch for dural closure. Furthermore, the dura mater in these infants is often dysplastic, thin, and lacking in collagenous integrity. When combined with the lack of robust paraspinal musculature to buttress the repair, the risk of CSF fistulization is inherently high. The leak is rarely a simple hole; it is often a complex, tortuous tract through friable tissue, making it prone to intermittent flow and difficult to identify visually.[16]

The term occult in this case refers to a leak that is radiologically invisible despite being clinically apparent. This paradox is best explained by the hydrodynamics of the fistula and the compliance of the infant's spine. Many postoperative leaks function via a valve mechanism. When the infant is supine and calm, as they are during an MRI or CT scan, the intrathecal pressure is relatively low. In this state, the granulation tissue or muscle flap overlying the fistula collapses, effectively sealing the tract. However, infants are dynamic systems. When the infant cries, strains, or performs a Valsalva maneuver, the intrathoracic pressure rises, causing a transient but

massive spike in intrathecal pressure.[17] This pressure overcomes the opening resistance of the valve, causing a spurt of CSF. Standard anatomical imaging fails to capture this dynamic. CT Myelography is a temporal snapshot; it captures the anatomy in a fraction of a second. If the infant is not straining at that exact moment of image acquisition, the contrast media may not extravasate, leading to a false negative. Furthermore, the volume of fluid in the track may be microscopic, below the spatial resolution of the scanner, yet sufficient to maintain a patent fistula that prevents wound healing.

Magnetic resonance imaging is universally accepted as the gold standard for defining neural anatomy, yet in this specific postoperative context, it failed. This failure is rooted in the physics of proton spin relaxation. MRI relies on the T2 relaxation times of protons to generate signal contrast.[18] On T2-weighted sequences, free water (CSF) has a long relaxation time and appears hyperintense (bright). However, the postoperative surgical bed is a chaotic environment. It contains serous fluid, postoperative edema, dissolving hematomas, and hemostatic agents such as gelatin sponges or oxidized cellulose. All these substances contain protons with T2 relaxation times that overlap significantly with those of CSF. Consequently, a pocket of bright signal on an MRI could be a static seroma, a piece of wet Gelfoam, or an active CSF leak. The MRI scanner cannot distinguish between these entities because it visualizes the *presence* of protons, not their origin or flow. In this case, the MRI likely showed fluid signal in the soft tissues, but the radiologist could not definitively state whether this was a contained postoperative collection or an active fistula communicating with the thecal sac. This ambiguity inevitably leads to clinical indecision or blind surgical exploration.[19]

Radionuclide cisternography utilizing Tc-99m DTPA operates on a fundamentally different physical principle: tracer kinetics and compartmentalization. DTPA (Diethylenetriaminepentaacetic acid) is a hydrophilic chelating agent that, when injected intrathecally, mixes freely with CSF and diffuses throughout the subarachnoid space. It does not cross the blood-brain barrier significantly and is cleared via arachnoid granulations and, to a lesser extent, transependymal flow.[20] The diagnostic power lies in the fact that the radiotracer is biologically alien to the soft tissues. If Tc-99m is detected within the paraspinal muscles or subcutaneous fat, it can only have arrived there via a physical breach in the dura. This effectively yields a background signal of zero in healthy tissue, providing an infinite contrast-to-noise ratio for the leak. Even a microscopic volume of extravasated fluid, if accumulated over the duration of the scan, becomes visible. However, traditional planar scintigraphy failed in this case, a finding that is instructive. In a 5-month-old infant, the anatomical distance between the spinal canal and the kidneys/bladder is only a few centimeters. Tc-99m DTPA is cleared renally. On a 2D planar image, the intense gamma photon emission from the bladder shines through and obliterates the much weaker signal from the spine. This is a classic limitation of projection imaging—the collapse of 3D anatomy into a 2D plane results in superposition artifacts.

Hybrid SPECT/CT overcomes this limitation through two distinct physical mechanisms: Tomographic Separation (SPECT): By rotating the gamma camera detectors 360 degrees around the patient, the system acquires data from multiple angles. Iterative reconstruction algorithms (such as OSEM - Ordered Subset Expectation Maximization) then mathematically separate the bladder activity from the spinal activity in 3D space. This removes the shine-through artifact, revealing the faint tracer activity in the fistula that was previously hidden by the bladder's glare. Anatomical Localization (CT): The nuclear image provides a hot spot but has poor spatial resolution (approximately 7-10 mm). It can confirm a leak exists, but cannot tell the surgeon exactly where to cut. The integration of the CT component provides the bony and soft tissue roadmap. In this patient, the fusion image allowed us to say that the tracer is not just in the lumbar region; it is specifically tracking from the L5 lamina into the right multifidus muscle.

This distinction is vital because tracer activity in a nerve root sleeve (a normal variant) can mimic a leak on SPECT alone. The CT component confirms that the tracer is outside the anatomical confines of the nerve root, confirming pathology.[17,18]

The localization of the tracer to the multifidus muscle is a finding of particular surgical relevance. It implies that the leak did not track directly to the skin surface in a straight line. Instead, the fluid dissected along the path of least resistance into the muscle belly, creating a pseudomeningocele or a fluid reservoir within the muscle. From this reservoir, fluid would intermittently overflow and seep through the fascial planes to the skin incision. This explains why the initial bedside exploration failed. The surgeon was looking for a hole in the dura directly under the skin opening. However, the true defect was deep in the muscle, offset from the skin opening. The SPECT/CT provided the treasure map that allowed the surgeon to bypass the confusing granulation tissue and dissect directly to the intramuscular reservoir and the underlying dural defect. A primary ethical and safety concern in pediatric imaging is the stochastic risk of ionizing radiation. Critics might argue for the exclusive use of MRI to avoid this risk. However, the risk-benefit analysis in this scenario heavily favors SPECT/CT, provided strict technical protocols are followed.

We adhered to the ALARA (As Low As Reasonably Achievable) principle by utilizing a specific localization CT protocol. Standard diagnostic CT scans for adults use high tube voltages (120 kVp) and currents (100-300 mAs) to produce pristine images of soft tissue. For the purpose of hybrid fusion, such quality is unnecessary. We require only enough skeletal detail to localize the tracer. Therefore, we lowered the tube voltage to 80 kVp and used a modulated current of roughly 30 mAs. This reduced the radiation dose of the CT component significantly. The effective dose of the radiotracer (37 MBq of Tc-99m DTPA) combined with the low-dose CT is estimated to be approximately 1.5 mSv. To place this in context, this is comparable to roughly 6 months of natural background radiation. In contrast, the risk of an untreated CSF leak includes bacterial meningitis, which carries a high mortality rate and a significant risk of permanent neurological sequelae such as hearing loss, cognitive delay, and hydrocephalus. Furthermore, a negative MRI often leads to blind surgical exploration, which carries risks of prolonged anesthesia, blood loss, and iatrogenic nerve injury. When viewed through this lens, the minimal radiation exposure from the SPECT/CT is a justified investment in the patient's long-term safety.

Another technical triumph in this case was the avoidance of general anesthesia. Pediatric SPECT/CT is notoriously sensitive to motion artifacts. If the patient moves between the SPECT acquisition and the CT acquisition, the fusion will be misregistered, potentially leading to surgical errors (e.g., localizing the leak to the wrong vertebra). In many centers, this necessitates intubation and anesthesia. We utilized a feed and bundle technique, capitalizing on the post-prandial somnolence of infants, combined with a vacuum-fixation mattress. This achieved adequate immobilization for the 20-minute scan duration without the respiratory risks associated with anesthesia in a prone infant. This protocol demonstrates that high-quality molecular imaging is feasible in infants without the heavy logistical and safety burden of anesthesia. The validity of the study depended on identifying potential pitfalls. One common error in cisternography is the epidural injection of the tracer. If the lumbar puncture needle does not fully enter the subarachnoid space, the tracer is deposited in the epidural fat. This results in slow, blunted absorption and can mimic a leak or fail to ascend to the site of pathology. We mitigated this by confirming free flow of CSF before injection and verifying the ascent of the tracer to the basal cisterns on the 1-hour images. Another potential pitfall is the degradation of the radiolabel. If the Tc-99m dissociates from the DTPA molecule, free pertechnetate is released. Pertechnetate is actively taken up by the thyroid and gastric mucosa and is excreted by the kidneys. High levels of free pertechnetate degrade image quality and increase

background noise. Our strict quality control, ensuring >98% radiochemical purity, was essential for the clarity of the final images.[19,20]

4. Conclusion

This case validates the pivotal role of Tc-99m DTPA Hybrid SPECT/CT Cisternography in the management of complex pediatric spinal complications. When anatomical imaging is rendered inconclusive by postoperative artifacts or intermittent flow dynamics, molecular imaging serves as the definitive problem-solving tool. We propose the following diagnostic algorithm for postoperative infants with suspected CSF leaks: First Line: Clinical assessment and MRI. This is non-invasive and provides excellent anatomical detail; Second Line: If MRI is negative or equivocal but clinical suspicion remains high (persistent discharge or collection), proceed directly to Hybrid SPECT/CT; Protocol: Utilize a low-dose CT component and delayed imaging (3-4 hours) to maximize the detection of slow leaks. Ensure pediatric-specific immobilization to avoid anesthesia. By adopting this precision medicine approach, clinicians can convert occult diagnostic challenges into clear surgical targets. The ability to visualize the physiology of the leak—not just the anatomy of the spine—allows for targeted, minimally invasive revision strategies. This significantly reduces morbidity, shortens hospital stays, prevents the devastating infectious complications associated with persistent CSF fistulas, and ultimately preserves the neurological potential of these vulnerable infants. The integration of SPECT/CT into the pediatric neurosurgical workflow represents a critical advancement in the standard of care for spinal dysraphism.

5. References

1. Taguchi Y, Takashima S, Konishi H, Tanaka K. SPECT/CT fusion imaging by radionuclide cisternography in intracranial hypotension. Intern Med. 2011; 50(20): 2433–4.
2. Bulman JC, Wachsmann J, Peng F. Asymmetric radiotracer activity of enlarged cerebral spinal fluid space on radionuclide cisternography with SPET/CT. Hell J Nucl Med. 2016; 19(3): 269–71.
3. Vamadevan S, Le K, Bui C, Mansberg R. Incidental 99mTc-DTPA uptake in Tarlov cysts on radionuclide SPECT/CT cisternography. Clin Nucl Med. 2017; 42(4): 287–8.
4. Jo N, Edhayan G, Owji S, Villanueva-Meyer J, Bhargava P. Detection of malpositioned VP shunt catheter by radionuclide CSF cisternography. Clin Nucl Med. 2023; 48(3): e110–1.
5. Freesmeyer M, Schwab M, Besteher B, Gröber S, Waschke A, Drescher R. High-resolution PET cisternography with 64Cu-DOTA for CSF leak detection. Clin Nucl Med. 2019; 44(9): 735–7.
6. Madhavan AA, Wood CP, Aksamit AJ, Schwartz KM, Atkinson JL, Kumar N. Superficial siderosis associated with an iatrogenic posterior fossa dural leak identified on CT cisternography. Neuroradiol J. 2022; 35(3): 403–7.
7. Barral CM, Lemos TR, Nunes SS, Sanches SMD. The value of radionuclide cisternography in a case of spontaneous cerebrospinal leak. World J Nucl Med. 2022; 21(2): 152–5.
8. García-Megias I, Cabada-Del Rio AM, Bonilla-Plaza J-A, Cruz Montijano M, García-Vicente AM. SPECT/CT as gatekeeper for extrathecal administration on 99mTc-DTPA cisternography. Clin Nucl Med. 2025.
9. Gedik GK, Uğur O, Atilla B, Pekmezci M, Yildirim M, Seven B, et al. Comparison of extraarticular leakage values of radiopharmaceuticals used for radionuclide synovectomy. Ann Nucl Med. 2006; 20(3): 183–8.
10. Sakurai K, Nishio M, Sasaki S, Ogino H, Tohyama J, Yamada K, et al. Postpuncture CSF leakage: a potential pitfall of radionuclide

cisternography. Neurology. 2010; 75(19): 1730–4.
11. Novotny C, Pötzi C, Asenbaum S, Peloschek P, Suess E, Hoffmann M. SPECT/CT fusion imaging in radionuclide cisternography for localization of liquor leakage sites. J Neuroimaging. 2009; 19(3): 227–34.
12. Gulaldi NC, Aras O, Gordon LL, Steenburg S. Ventriculoperitoneal shunt leakage into a breast implant demonstrated by radionuclide cisternography. Clin Nucl Med. 2011; 36(12): 1127–8.
13. Chiu Y-L, Tsay D-G, Hu C, Wu C-S, Du W-N, Peng N-J. Intrathoracic renal ectopia mimicking CSF leakage on radionuclide cisternography demonstrated by SPECT/CT. Clin Nucl Med. 2012; 37(1): 93–4.
14. Takahashi M, Momose T, Kameyama M, Mizuno S, Kumakura Y, Ohtomo K. Detection of cerebrospinal fluid leakage in intracranial hypotension with radionuclide cisternography and blood activity monitoring. Ann Nucl Med. 2005; 19(4): 339–43.
15. Ak I, Uslu I. Bowel visualization as a sign of cerebrospinal fluid leakage on radionuclide cisternography. Clin Nucl Med. 2008; 33(11): 811–2.
16. Morioka T, Aoki T, Tomoda Y, Takahashi H, Kakeda S, Takeshita I, et al. Cerebrospinal fluid leakage in intracranial hypotension syndrome: usefulness of indirect findings in radionuclide cisternography for detection and treatment monitoring. Clin Nucl Med. 2008; 33(3): 181–5.
17. Semirgin SU, Basoglu T, Cokluk C, Sahin Z. Radionuclide imaging with SPECT/CT in suspected cerebrospinal fluid leakage. Clin Nucl Med. 2012; 37(3): 289–92.
18. Arai H, Yamamoto Y, Maeda Y, Aga F, Dobashi H, Nishiyama Y. SPET/CT imaging in radionuclide cisternography to detect cerebrospinal fluid leakage in spontaneous intracranial hypotension associated with SLE. Eur J Nucl Med Mol Imaging. 2012; 39(7): 1225–6.
19. Nursal GN, Yapar AF. Demonstration of cerebrospinal fluid leakage on radionuclide cisternography by SPECT/CT. Clin Nucl Med. 2015; 40(1): e55-7.
20. Chen M-Y, Wang Y-F, Peng N-J, Lee T-H. Radionuclide cisternography revealed neck cyst formed by cerebrospinal fluid leakage after cervical spine surgery. Clin Nucl Med. 2026; 51(1): 63–4.